ELSEVIER

Ecological Modelling 82 (1995) 75–91

ECOLOGICAL MODELLING

Spatial model error analysis using autocorrelation indices

Geoffrey M. Henebry

Division of Biology, Kansas State University, Manhattan, KS 66506, USA

Received 3 September 1993; accepted 12 April 1994

Abstract

No standard techniques yet exist for assessing the predictive performance of models that simulate spatially-explicit processes. Spatial simulation models generate autocorrelation patterns that are a critical aspect of model prediction. These patterns can be quantified using spatial (Moran's *I*) and spatio-temporal (Griffith's *STI*) autocorrelation indices. A method of error analysis for spatial simulation models is demonstrated using autocorrelation indices to distinguish among the effects of parameter uncertainty on a stochastic spatial simulation of seed dispersal. The resulting autocorrelation patterns of state variables display a range of nonlinear, counterintuitive effects. In contrast to techniques proposed for spatial model error analysis (contagion, spatial predictability, adjacency, multiple resolution procedure, fractal dimension, interface), autocorrelation indices can be used with interval-scaled data and have well-defined sampling distributions that enable significance testing.

Keywords: Autocorrelation; Error analysis; Spatial patterns; Uncertainty analysis

1. Introduction

A wide range of environmental management issues involve ecological processes that are both spatially-explicit and scale-dependent, e.g., habitat fragmentation, biodiversity preservation, land use, and demographic patterns. Cross-disciplinary fields, such as landscape ecology (Forman and Godron, 1986; Turner, 1989) and conservation biology (Soulé, 1986,1991), have emerged to address some of these problems through both basic and applied research. Practical solutions will depend upon monitoring strategies that, in turn, require the development of methods for quantifying landscape change. Simulation models that incorporate spatial as well as temporal dynamics can serve as a framework for quantifying landscape change (Costanza et al., 1990).

Spatially-explicit simulation of ecological processes poses a variety of technical obstacles, not the least of which is a lack of model diagnostic procedures (error, uncertainty, and sensitivity analyses) that can properly quantify the spatial and spatio-temporal correlation patterns that emerge in simulation. This paper introduces the use of the autocorrelation indices for spatial model error analysis, describes their mathematical formulation, and demonstrates their efficacy using a stochastic spatial simulation of seed dispersal.

1.1. The challenge of spatial simulation

Ecological simulation models that incorporate spatial processes are relatively rare (Sklar and Costanza, 1991). This situation can be traced to

SSDI 0304-3800(94)00074-R

three principal causes: (1) the computational complexity of spatial processes; (2) a broad range of scaling issues, from functional rescaling to data management; and (3) the relative paucity of statistical theory and methods for spatial data.

First, computers based on the traditional von Neumann architecture are ill-suited for simulating data-parallel contingent processes (Hillis, 1986; Hillis and Boghosian, 1993). Yet most computers currently available to researchers follow this paradigm. Accordingly, the more popular computer languages (FORTRAN, C, Pascal) and the majority of extant application codes were developed for the von Neumann architecture. Recent and continuing developments in hardware and software promise to attenuate this constraint on spatial simulation (Costanza and Maxwell, 1991; Golub, 1993). Nevertheless, the computational complexity of ecological spatial models is driven by multiple temporally-nested processes generating spatially-explicit patterns that, in turn, affect those processes, often at multiple scales. This characteristic behavior of spatial simulation, multiple contingently-interacting scales, will likely remain difficult to formalize efficiently either in software or hardware; thus, spatial simulations will continue to present a significant computational burden.

Second, an active area of research critical to the success of spatial simulation modelling concerns the scaling of data and processes to reflect varying degrees of spatial, temporal, and functional resolution (Rosswall et al., 1988; King, 1991). A firm theoretical foundation for rescaling procedures is essential for simulation models to exploit effectively the data-rich technologies of remote sensing and Geographic Information Systems (GIS).

Some scaling properties of data have been studied for over a decade in quantitative geography as the Modifiable Unit Area problem (Openshaw, 1977; Openshaw and Taylor, 1981) and in theoretical ecology as the twin problems of "transmutation across scales" (O'Neill, 1979) and aggregation error (Cale and Odell, 1980; Gardner et al., 1982). Recent research has demonstrated that even in the simplest case, viz., a stationary Gaussian spatial process on a regular lattice, rescaling by either averaging or summation of the original data leads to nonstationarity and bias in the distribution of the rescaled data (Arbia, 1989). Similarly, functional representations involving nonlinear relationships can be altered significantly by these simple rescaling procedures (King et al., 1991; Rastetter et al., 1992).

Third, the very nature of spatial processes poses significant challenges to the development of statistical estimation and inference procedures (Ripley, 1988; Cressie, 1991). Ripley (1988) lists salient features of spatial systems that confound conventional statistical theory:

- no a priori causal ordering among observations;
- edge effects and boundary conditions;
- asymptotic arguments about distributions cannot include ratios of infinities;
- long-range dependence among observations and its connection with phase transitions;
- maximum likelihood methods of parameter estimation that require iterative nonlinear solutions or too many combinatorial terms;
- the many forms of nonstationarity (patchiness, anisotropies, nested effects, trends, periodicities) are often simultaneously present; and
- discretization from sampling can distort data attributes and induce nonstationarity, e.g., "bulking" in soil science and "regularization" in remote sensing.

These same characteristics also create problems for simulation modelling. Parameterization and calibration data for a model must be carefully managed (Cressie, 1991). Design of effective sampling schemes require exploratory data analysis (1) to gauge the range of spatial and temporal scales across which variation is dominant and (2) to determine the grain size of the simulation unit.

Estimation of spatially-distributed parameters and functions requires decomposition into elements of lower frequency (trends, gradients) and higher frequency (local interactions, noise). Processes can then be classified as reactive or interactive (Cliff and Ord, 1981a). The reactive process is governed solely by factors within its simulation unit (gridcell or polygon); whereas the interactive process influences and/or is influenced by other processes within some appropriately de-

fined neighborhood. The dynamics of interactive spatial processes can unfold into complex spatio-temporal behavior, e.g., traveling waves in diffusion-reaction systems (Murray, 1990). Nested hierarchies of reactive and interactive processes can further complicate model behavior. Even in the absence of emergent macroscopic behavior, interactive processes generate complicated patterns of spatio-temporal autocorrelation.

Autocorrelation is a characteristic of data derived from a process that is articulated in one or more dimensions and it describes the error structure of the data. Generally, if adjacent or proximate observations exhibit similar deviations from the mean, the data are autocorrelated. In positively (negatively) autocorrelated data the deviations are less (more) variable than would be expected in random residuals. Autocorrelation can pose a significant problem in analysis of simulation runs. When applying statistical procedures that assume independently-distributed errors, the risk of making a Type I error is increased when data are positively autocorrelated and a Type II error when data are negatively autocorrelated (Ripley, 1988). Error propagation techniques based on first-order Taylor expansions (Scavia et al., 1981; Beck, 1987) are similarly confounded by autocorrelation.

Of the many challenges to spatial simulation modelling, autocorrelation is among the more difficult to deal with using traditional model diagnostics and analyses. Autocorrelation, however, is an intrinsic property of spatial processes that is readily quantifiable. Thus, inclusion of measures of autocorrelation into error and uncertainty analyses provides a mechanism to assess the uniquely spatial aspects of the spatial model.

1.2. Autocorrelation and error analysis

A suite of standard techniques exists for the evaluation of spatially-aggregated, temporally-articulated models, including Monte Carlo uncertainty analysis (O'Neill et al., 1986; Warwick and Cale, 1986), first-order uncertainty analysis (Scavia et al., 1981; Chadderton et al., 1982), and regionalized sensitivity analysis (Hornberger and Spear, 1981). Assessing the performance of spatially-explicit models is a more subtle problem. Lacking a priori causal ordering, spatial processes can generate spatio-temporal as well as temporal feedback loops, thus inducing complex patterns of autocorrelation that hinder statistical inference (Ripley, 1988).

Quantitative geography has addressed the issue of spatial autocorrelation in some detail (Cliff and Ord, 1981a; Upton and Fingleton, 1985); however, the methodological focus is typically retrospective, e.g., fitting linear stochastic processes to small samples of historical data to enable forecasting and planning (Anselin, 1988). Epidemiology, on the other hand, uses statistical procedures that detect clustering in space and time, from which to infer a common etiological source (Knox, 1964; Mantel, 1967; Klauber, 1975; Selvin, 1991).

The perspective of ecology is necessarily different. Contemporary ecology aims to understand pattern in terms of process and how pattern, in turn, affects process (Cale et al., 1989; Turner, 1989). Ecological modelling currently emphasizes a bottom-up, hierarchical approach to simulation: relevant patterns emerge as the behaviors of many interacting smaller-scale processes are constrained by larger-scale phenomena (O'Neill et al., 1986; Huston et al., 1988).

The object of simulating ecological phenomena is to replicate observed patterns of system dynamics. Typically, these patterns involve the distribution and abundance of state variables in time and, less often, in space. Implicit in the use of a spatial simulation model is the objective of capturing patterns generated by the spatially-explicit interactions. If a project warrants the computational burden of spatial simulations, then model evaluation should include error analyses that focus on those aspects that distinguish spatial modelling from aspatial modelling: the spatio-temporal patterns of mean, variance, and autocorrelation. Accordingly, model evaluation requires techniques to characterize spatio-temporal patterns that should be (1) statistically well-defined in the sense of being able to test hypotheses, (2) sensitive to scale effects (i.e. changes in grain and/or extent), and (3) computationally efficient. Autocorrelation indices can fulfill these requirements.

1.3. Measuring spatial autocorrelation

A general measure of spatial interaction requires a few structuring assumptions in the form of a weighting scheme, W. Understanding interaction as a function of proximity or, more simply, contiguity leads to the concept of a bounded neighborhood of spatial influence, $W = \sum_j \sum_i w_{ij}$, where i and j are spatial indices. A further simplification views spatial interactions within the neighborhood as mutually and symmetrically related, i.e., $w_{ij} = w_{ji}$. While this assumption usually does not pertain to the mean values in gradient-driven systems, it often holds for the deviations from those means. Moreover, this assumption speaks to relatedness, not causality. Weaving together the concepts of spatial weighting, local (neighborhood) deviations, and regional variance, a measure of spatial autocorrelation can be formulated.

Moran's I is an index that gauges the intensity of spatial autocorrelation in interval-scaled data as a function of lag neighborhood (Moran 1950; Sokal and Oden, 1978a,b; Cliff and Ord, 1981a). The form of the index is a covariance/variance ratio with a weighting scheme based on spatially-symmetric interactions:

$$I = \left(n \sum_{j=1}^{n} \sum_{i=1}^{n} w_{ij} z_i z_j \right) \left(S_0 \sum_{i=1}^{n} z_i^2 \right)^{-1} \quad (1)$$

where n is the number of areal units, w_{ij} is a spatial weighting, z is the deviation from mean, and S_0 is the sum of the weighting matrix. The expected value of the index is a negative reciprocal function of the number of sampling units: $-(n-1)^{-1}$. Variance of I can be calculated using either of two distributional assumptions about the data (Cliff and Ord, 1981a). Under the normality assumption, the observed data map is the result of n independent samples from one or more normal distributions. Under the randomization assumption, the observed data map is one permutation out of $n!$ possible maps given the collection of observed data values. Fortunately, the sampling distribution is asymptotically normal under either assumption. Even small (10×10) regular grids yield practically indistinguishable values for I. Significance tests can be based on z-scores (standard normal deviates). Versions of Moran's I to accommodate higher lag-orders, ordinal data, and regression residuals are available (Cliff and Ord 1981a; Upton and Fingleton 1985).

Moran's I resembles the classic Pearson product-moment correlation coefficient. However, it should not be interpreted as a direct estimate of the correlation parameter: a particular spatial stochastic model, such as a first-order conditional autoregressive (spatial Markov) model, must first be specified to enable parameter estimation. Parameter estimation for spatial processes is usually not a trivial exercise, involving solutions to implicit nonlinear equations (Cliff and Ord, 1981a; Cressie, 1991).

Calculation of Moran's I is computationally straightforward, especially for regular gridcell (lattice) data for which standard assignments of a cell's neighborhood exist. In gridcell systems it is convenient to use chess analogies and compass directions to define three principal neighborhoods: (1) the rook's influence extends along orthogonal axes, N–E–S–W; (2) the bishop's influence is the rook's neighborhood rotated 45 degrees, NW–NE–SE–SW; and (3) the queen's influence is the compound of both rook and bishop, NW–N–NE–E–SE–S–SW–W. First-order autocorrelation is measured as a function of nearest neighbors; higher-order autocorrelation is measured as a function of more distant neighbors along the defining axes.

Once the neighborhood is defined, weights must be assigned to the neighbors. The simplest weighting scheme uses binary (0,1) weights based on contiguity. Because higher-order neighborhoods include gridcells not located along the principal axes, classes based on distance measures (e.g., Euclidean) can be used to assign contiguity. Many other weighting schemes are possible. Based on studies of the asymptotic relative efficiency (ARE) of Moran's I, Cliff and Ord (1981a) recommend that "the weights in the test statistic should correspond to the dependence structure postulated in the alternative hypothesis" (p. 178). For example, if the alternative hypothesis is nearest-neighbor isotropic influence, then binary weighting of the queen's neighborhood is appropriate.

Complications arise for the specification of the weighting matrix in polygonal maps due to the intrinsic lack of causal directionality in spatial systems. The question "who is neighbor of whom?" is much less clear but differential weighting schemes can be more useful. Chou et al. (1990), in a study of spatial autocorrelation of wildfire distribution, examined how different weighting schemes affected the explanatory ability of Moran's I in a logistic regression of polygonal GIS map layers. They found that binary contiguity weighting was most informative. In absence of a priori information that could order neighborhood connections, such as hydraulic or elevational gradients, a binary contiguity weighting matrix is an appropriate preliminary choice.

1.4. Measuring spatio-temporal autocorrelation

As with measuring spatial interaction, an assessment of spatio-temporal interaction requires structuring assumptions about the weighting matrix and neighborhood relatedness. Let us now assume an asymmetry in spatial interactions induced by a temporal lag, i.e., $w_{ijt} \neq w_{jit-1}$. The topology of spatial neighborhood is similar to that of the spatial autocorrelation index, except for its temporal displacement. The interaction neighborhood is thus a double cone in space–time with the vertex at the current position, one cone of influence flowing in from the past, and another extending out into the future.

The Space–Time Index (*STI*) is one of several related measures that have been proposed for assessing spatio-temporal autocorrelation (Knox, 1964; Mantel, 1967; Cliff and Ord, 1981b; Griffith, 1981). The formulation by Griffith (1981) combines the Moran index with the Durbin–Watson statistic, a widely-used diagnostic to assess serial independence in regression residuals, to yield a first-order *STI*:

$$STI = (nT - n)\left(\sum_{t=2}^{T} \sum_{j=1}^{n} \sum_{i=1}^{n} w_{ijt-1} z_{it} z_{jt-1} \right) \times \left(\sum_{t=2}^{T} \sum_{j=1}^{n} \sum_{i=1}^{n} w_{ijt-1} \sum_{t=1}^{T} \sum_{i=1}^{n} z_{it}^2 \right)^{-1} \quad (2)$$

where n is the number of areal units, T is the number of temporal units, w_{ijt} is a spatio-temporal weighting, and z is the deviation from the space–time mean. The expected value of *STI* is similar to Moran's index, a negative reciprocal function of the number of sampling units: $-(T-1)*[T*(nT-1)]^{-1}$. Under the normality assumption, the variance of *STI* can be calculated without further parameter estimation (see Appendix). Although the assumption of normality has been shown to be tenuous for space–time clustering statistics based on binary data (Siemiatycki, 1978; Barbour and Eagleson, 1986), sufficiently large space–time sample sizes of interval-scaled variables enable the invocation of the Central Limit Theorem to justify the normality assumption (Cliff and Ord, 1981b; Griffith 1981).

A major advantage of the autocorrelation indices is that the first and second moments of their sampling distributions are well-defined. Accordingly, the statistical significance of spatial and spatio-temporal autocorrelation patterns found in model generated maps can be directly assessed using standard normal deviates (z-scores). While neither I nor *STI* is a direct parameter estimate, these indices can provide a relative measure of the intensity of autocorrelation, which enables their use as model diagnostics in error analyses.

2. Methods

Models seek to reproduce observed patterns of state variables. In terms of error analysis, a spatial simulation model can be viewed as generating a spatial component (a distribution map of values at each timestep), a temporal component (a time-series of mean map values), and a spatio-temporal component (a time-series of maps of values). Model predictions can fail to correspond to the observed patterns in any combination of these components. If the observed patterns are assumed to be produced by systems of processes that include stochastic elements, then a single set of observed patterns is an inappropriate refer-

ence for error analysis. Instead, analyses must compare moments of the distributions of error components. The basic approach is first to posit a set of "truths" by generating reference distributions from the simulation model and then to examine deviations from these referents at various levels and combinations of parameter uncertainty using a Monte Carlo simulation strategy. The simulation vehicle used here is a simple stochastic model of seed dispersal that I developed specifically for generating complicated correlational patterns in space and time. A detailed account of the error analysis methodology follows a description of the model.

2.1. Model description

The operating space of the model is a series of matrices each of which correspond to a hypothetical landscape divided into a regular 30×30 square grid. One matrix holds the plant population of the current generation; another matrix holds the current seed population. Additional matrices can be used to introduce temporal lag effects, such as perennials or seed bank dynamics, as well as abiotic potential surfaces, such as soil water, soil temperature, and wind direction. Results reported here used the simplest configuration of two matrices under isotropic environmental conditions.

Model dynamics are biphasic: plants can produce seeds which, in turn, can yield plants (Fig. 1). In the basic simulation scenario, the model is initialized by a random distribution of plants across the gridscape. Seed production per plant per gridcell is affected by the neighborhood (in-

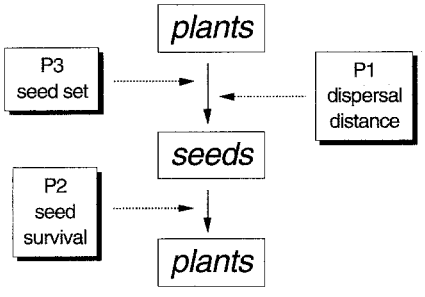

Fig. 1. Schematic of seed dispersal model with perturbed parameters highlighted.

ter-cell) plant density using a density-dependent multiplier described below. Each seed from each plant is then dispersed in an uniformly random direction to a negative-exponential random distance. During dispersal, the gridscape has periodic boundary conditions (a torus). Intra-cell seed populations were similarly adjusted by the density-dependent multiplier to determine the survival of seeds into mature plants. One generation is thus completed.

The density-dependent multiplier v_i is a piecewise-continuous threshold function that determines the proportion of the population surviving *si* after the *i*th state variable has exceeded a specific threshold T_i:

$$\text{if } N_i \leq T_i, \text{ then } v_i = 1$$

$$\text{else } v_i = \left[1 - \left(B \cdot (N_i - T_i)^r \cdot (N_i)^{-r}\right)^q\right]_+$$

The parameters B, q, and r define how drastically the populations are diminished by Eq. 3 after the threshold T_i has been exceeded. The bracketed term carrying the positive subscript

Table 1
Model parameters used in reference simulations

Parameter explanation	Value
Mean for maximum seed set per plant	30 seeds
CV for maximum seed set per plant	20%
Plant population threshold for density-dependent function affecting seed set	20 plants
CV for plant population threshold	20%
Seed population threshold for density-dependent function affecting seed survival	(Mean seed set)*0.25
CV for seed population threshold	10%
Mean seed dispersal distance	5 gridcells
CV for seed dispersal distance	50%

evaluates to a non-zero term only for positive values; the term is mapped to zero for negative values.

2.2. A method for spatial model error analysis

The method developed here to conduct spatial model error analysis is conceptually simple but computationally involved. The first stage is identifying which aspects of the model are to be varied and which measures of model output are to be analyzed. Nominal model parameters and initial conditions for the reference set can then be specified and reference distributions can be generated.

A set of reference distributions were formed by 100 Monte Carlo simulations using nominal model parameters (Table 1) run to 50 generations. Several measures of model output for seed and plant populations were calculated during each simulation: aspatial abundance (mean and standard deviation); spatial autocorrelation (Moran's *I*); and spatio-temporal autocorrelation (Griffith's *STI*). The empirical sampling distributions of these measures served as reference distributions and were summarized by mean, standard deviation, standard error (SE), coefficient of variation (CV), and median.

In the second stage, three model parameters received random variation: (1) mean seed dispersal distance; (2) population threshold for density-dependent function governing seed survival into mature reproductive plants (seed survival); and (3) population threshold for density-dependent function governing plant reproductive effort (seed set). These parameters were subjected to random perturbations at levels of 10%, 20%, and 40% CV in separate Monte Carlo runs. Perturbations were drawn from a normal distribution truncated at ± 3 standard deviations. As the intent of this study was to focus on the efficacy of the error analysis technique and not model performance per se, the initial distribution of plants across the gridscape was not varied. I explored the effects of parameter uncertainty on the spatial and spatio-temporal autocorrelation patterns by systematically varying which parameters were subject to perturbation (Table 2). A set of distributions was generated (100 Monte Carlo runs at 50 timesteps) for each of these perturbed configurations at each uncertainty level. The same random number seed was used for each configuration-by-uncertainty Monte Carlo suite to facilitate comparisons. Each distribution for each output measure was then summarized by mean, standard deviation, SE, CV, and median.

Table 2
Model configurations used in simulations

Model configuration	Parameters perturbed
000	None: Reference run
001	Seed set
010	Seed survival
100	Dispersal distance
011	Seed set; seed survival
101	Dispersal distance; seed set
110	Dispersal distance; seed survival
111	All: dispersal, survival, set

In the third stage summary statistics from reference and perturbation sets are reduced and compared. Time series of vectors are formed using comparable state variable statistics, e.g., mean abundance for seeds and plants, and their Euclidean distance from the origin are calculated with plant and seed components being equally weighted. This procedure enables all state variables to be assessed simultaneously. Abundance and spatial autocorrelation distances are then integrated through time, from generation 5 to 50, thereby avoiding the initial transient. The *STI* measure incorporates the temporal dimension in its definition and was calculated from generation 5 to 50. At this point, there are time-integrated distances for the summary statistics (mean, median, CV, SE) of model output measures (abundance, Moran's *I*, Griffith's *STI*) for 22 model configurations (7 perturbation sets by 3 CV levels plus 1 reference set). Sets of perturbed distances are then normalized against their corresponding reference set to quantify deviations in terms of percentage from reference.

The penultimate stage of the spatial model error analysis distinguished among model configurations on the basis of statistical error tolerances. Using the standard errors from the plant and seed sampling distributions, vectors repre-

senting ±2 SE were carried through calculations to yield approximate 95% confidence bounds for the deviation of integrated mean abundance, integrated mean spatial autocorrelation, and mean spatio-temporal autocorrelation. An alternative assessment strategy could employ user-defined error tolerances to evaluate the proportion of the model output distribution falls within the tolerance interval (Warwick and Cale, 1988; Henebry, 1989). This latter approach requires "reality filters", either external criteria (e.g., policy considerations) on acceptable model performance or prior knowledge (e.g., expert opinion) about the practical ecological significance of model predictions.

Finally, to assess the overall effect of uncertainty on the parameters and the model configurations, statistically significant deviations in the three measures were combined into a vector for each configuration-by-uncertainty combination and the Euclidean distance from the origin or significant absolute deviation (SAD) was calculated. The general effect of parameter uncertainty on model performance was alternatively assessed by viewing the model as a black-box filter through normalizing output uncertainty by input uncertainty (Henebry, 1989). The normalized time-integrated deviations in abundance and spatial autocorrelation CV, used as measures of output uncertainty, were divided by input uncertainty (10%, 20%, or 40% CV) to yield an uncertainty scaling factor (USF). Positive USF values denote amplification of uncertainty and negative USF values denote uncertainty attenuation. This procedure permits classification of the model as either a linear or nonlinear filter of uncertainty.

3. Results

3.1. Nominal model behavior

As the uncertainty analysis uses nominal model behavior as the reference case, it is first necessary to characterize that behavior and to establish that it converges to some basin of attraction. A key feature of the model is the negative relationship between plants and seeds that emerges from the interaction of density-dependent controls on both seed set and seed survival (Fig. 2). Fig. 3 displays phase plots of the means and CVs of abundance in plant and seed distribution maps during the 50 generation simulation period. Values are based on the means of 100 Monte Carlo realizations using the nominal parameters and have been normalized to the observed dynamic range to emphasize the initial transient and subsequent

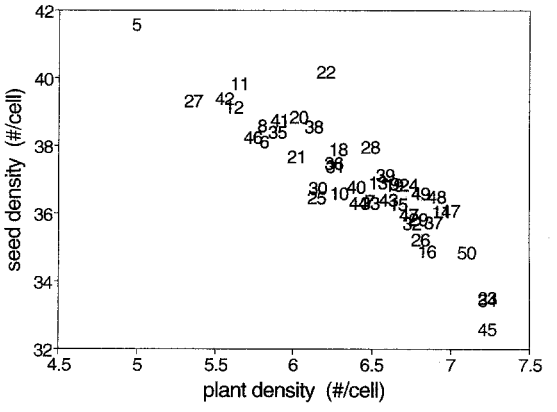

Fig. 2. Median seed and plant abundances during generations 5 to 50 of reference simulation. Numbers denote generation time.

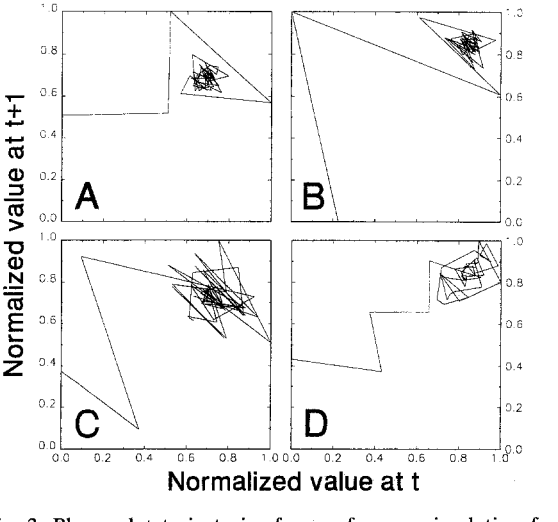

Fig. 3. Phase plot trajectories from reference simulation for (a) normalized mean plant abundance, (b) normalized mean seed abundance, (c) normalized CV of plant abundance, and (d) normalized CV of seed abundance.

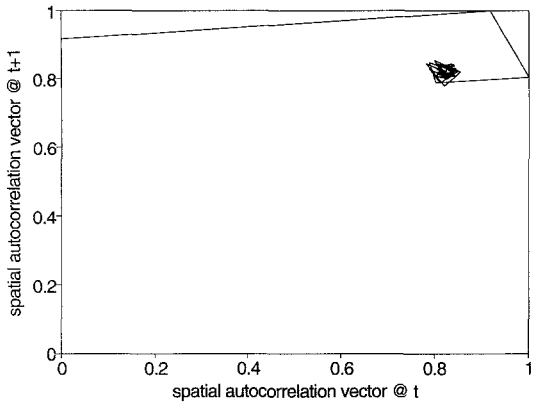

Fig. 4. Phase plot trajectory from reference simulation for the Euclidean distance of mean spatial autocorrelation vector calculated from plant and seed distribution maps using the queen's case of Moran's I at lag 1.

convergence to the attractor. As with the aspatial abundance levels, the spatial correlation structure of abundance maps converge toward an attractor (Fig. 4). Because data normalization obscures observed values, it is important to indicate the degree and direction of the autocorrelation indices. Spatial autocorrelation for plants and seeds was strongly positive; whereas, spatio-temporal autocorrelation was strongly negative, especially for plants.

3.2. Effects on separate measures

Before presenting the main results, let me reiterate the model configuration codes found in Table 2. Each code is a 3-bit sequence designated which parameters are subject to uncertainty. The first position (*100*) introduces uncertainty into the expected dispersal distance of seeds and thereby affects the spatial distribution of future plants; the second position (*010*) affects the survival of seeds within a gridcell and thereby the number of future plants in that gridcell; and the third position (*001*) affects the number of seeds to be produced by a plant within a gridcell and thereby the number of future plants in the gridcell's neighborhood. The effects of parameter uncertainty on model behavior are manifested differently depending upon which measure (aspatial abundance, spatial autocorrelation of abundance,

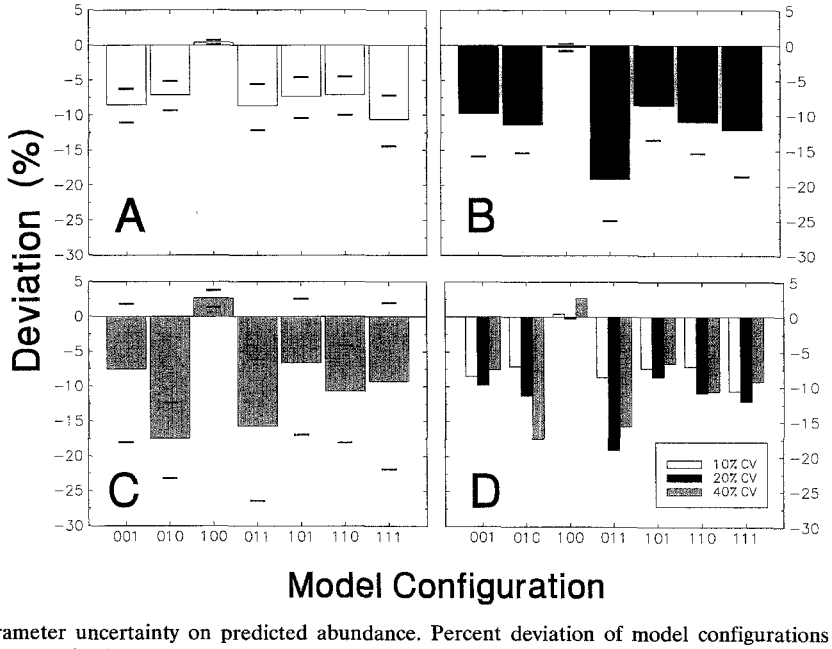

Fig. 5. Effect of parameter uncertainty on predicted abundance. Percent deviation of model configurations for time-integrated vectors of mean abundance (bar) and ±2 standard errors (lines) at uncertainty levels of (a) 10%, (b) 20%, (c) 40%, (d) altogether.

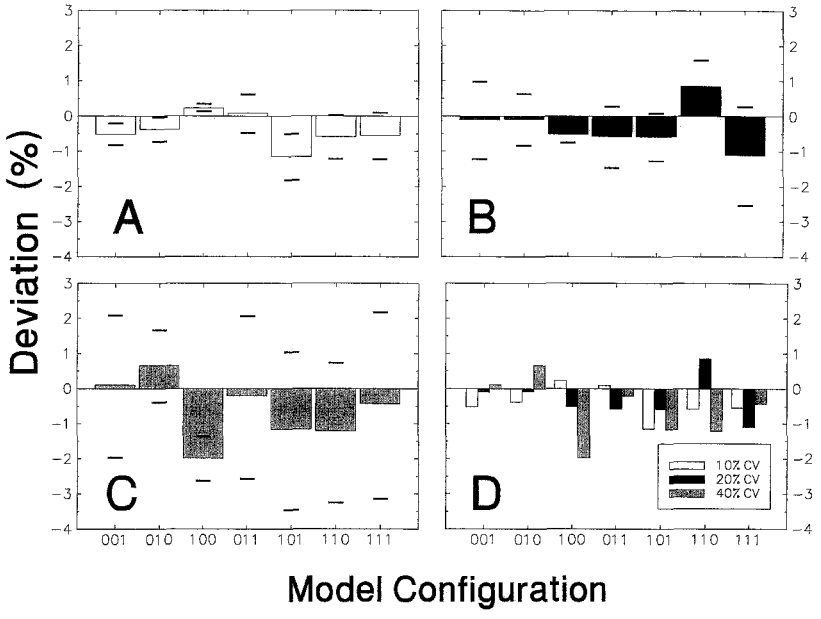

Fig. 6. Effect of parameter uncertainty on predicted spatial autocorrelation. Percent deviation of model configurations for time-integrated vectors of mean Moran's I (bar) and ± 2 standard errors (lines) at uncertainty levels of (a) 10%, (b) 20%, (c) 40%, (d) altogether.

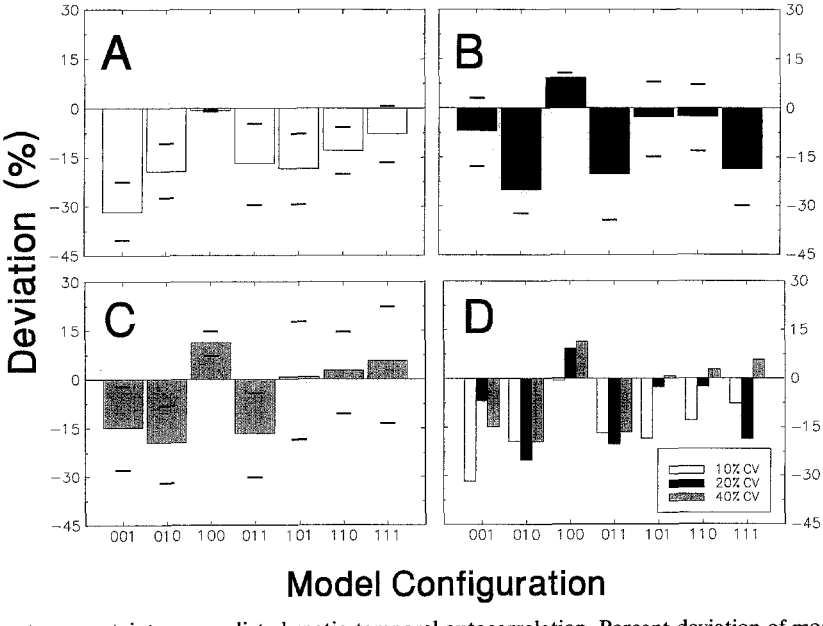

Fig. 7. Effect of parameter uncertainty on predicted spatio-temporal autocorrelation. Percent deviation of model configurations for time-integrated vectors of mean Griffith's *STI* (bar) and ± 2 standard errors (lines) at uncertainty levels of (a) 10%, (b) 20%, (c) 40%, (d) altogether.

or spatio-temporal autocorrelation of abundance) is used.

Parameter uncertainty lowers predicted abundances by 7 to 19% in most model configurations (Fig. 5). In the sole exception, configuration *100* in which only the dispersal distance is perturbed, there is a statistically significant but marginally positive effect at 10% and 40% CV and no significant effect at 20% CV. An increase in predicted abundances from an increase in variability of dispersal distance is expected where density-dependent controls are a function of local neighborhoods. For configurations with either density-dependent parameter, the attenuation of abundance is statistically significant at 10% and 20% CV (Fig. 5a,b) but at 40% CV (Fig. 5c) three of four configurations with parameter 3 (*001*, *101*, *111*), the density threshold for seed set, are not significantly different from the reference case. Parameter 2, the density threshold for seed survival, appears to give a linear response to parameter uncertainty (*010* in Fig. 5d); whereas, parameters 1 and 3 manifest nonlinear responses to increased parameter uncertainty (*001* and *100* in Fig. 5d). The dominant effect for interactions is nonlinear (*011*, *101*, *110*, *111* in Fig. 5d).

The effects on spatial autocorrelation are considerably less pronounced (Fig. 6), ranging from a maximum significant negative impact of 2% (*100* in Fig. 6c) to a maximum significant positive impact of less than 1% (*110* in Fig. 6b). Two-thirds of the configurations are not statistically different from the reference case. The effect on configuration *100*, however, is significant across uncertainty levels; as would be expected, variation in a spatial parameter translates into variation in spatial pattern. While most configurations exhibit a nonlinear response pattern across uncertainty levels (Fig. 6d), the general lack of significant differences from the reference make conclusions tenuous.

Spatio-temporal autocorrelation patterns exhibit both nonlinear responses and significant deviations under parameter uncertainty (Fig. 7). Low uncertainty applied to parameter 3 (*001* in Fig. 7a) yielded the maximum attenuation of more than 30% in spatio-temporal autocorrelation; whereas high uncertainty applied to parameter 1 (*100* in Fig 7c) amplified spatio-temporal autocorrelation by more than 10%. In contrast to the spatial autocorrelation patterns, two-thirds of the effects observed in spatio-temporal autocorrelation are significant. Moreover, the three configurations with consistently significant deviations (*010*, *100*, *011*) exhibit nonlinear responses to parameter uncertainty (Fig. 7d). At low uncertainty (10% CV) every configuration yields significant differences except for the fully perturbed case (*111*). As uncertainty level is increased, the configurations with an interaction involving parameter 1 (*101*, *110*, *111*) are less likely to be significantly different from the reference.

Table 3
Significant absolute deviations (SADs) from reference (*000*) for model configurations averaged across uncertainty levels. SADs derived from simulations for every configuration and from averaging single parameter deviations for multiple parameter configurations

Model configuration	Simulation SAD (%)	Averaged SAD (%)	Percent difference
010	24.7	–	–
011	23.2	21.9	5.4
001	19.1	–	–
111	16.4	17.0	−3.9
101	14.2	13.2	7.3
110	12.1	16.0	−31.8
100	7.3	–	–

3.3. Ranking overall effects

Using significant absolute deviations (SADs) the response of the model configurations to parameter uncertainty can be ranked by magnitude of deviation, thereby permitting a determination of parameter sensitivity (Table 3). The SADs calculated for each model configuration were averaged across uncertainty levels due to the nonlinearities observed in the separate measures (Figs. 5–7).

Considering first only those configurations with single perturbed parameters, the density threshold for seed survival (*010*), is the most sensitive to uncertainty (24.7%), followed closely by *001*, the density threshold for seed set (19.1%). The explicitly spatial parameter, mean seed dispersal

distance (*100*), ranks a distant third (7.3%). Considering all configurations, it is evident that variation in parameter 3 attenuates deviations contributed by variation in the other parameters, e.g., $110 \ll 011$. If the effects of uncertainty generated by each separate parameter are largely equivalent, then we may be able to predict the SADs for configurations with multiple perturbed parameters from a simple operation, such as averaging, on the appropriate single parameter SADs, e.g., $(001 + 100)/2 = 101$. Calculating SADs for multiple parameter configurations by this alternative averaging method yields estimates that are quite close (within 10%) to the SADs derived from the simulation results (Table 3). The notable exception to this trend is the SAD for configuration *110* which is overestimated by 31.8% using the averaging method. This substantial difference suggests a significant interaction between mean seed dispersal distance (parameter 1) and seed survival threshold (parameter 2). The interaction is understandable from the dynamics of the model (Fig. 1). Given a number of seeds to be distributed across an unsaturated toroidal habitat, a larger dispersal distance translates into a more even distribution of seeds and eventually plants across the gridscape. A more even distribution will lead to fewer local extinctions. This interaction is apparently neutralized by perturbations to the seed set threshold (parameter 3); the difference between simulation and averaged SADs for *111* is relatively small, −3.9% (Table 3). Again this is understandable given the model structure: local variations in seed set can translate into global patchiness once the seeds are broadcast.

According to SAD patterns, the population threshold for seed survival (parameter 2) appears to be the most sensitive and the mean seed dispersal distance (parameter 1) is the most robust of the model parameters examined.

3.4. Uncertainty scaling

Given a certain quantity of uncertainty introduced to the model, what quantity of uncertainty is generated? The intuitive expectation is that increasing input uncertainty leads to increasing output uncertainty. The results obtained from this simple spatial simulation model are counterintuitive (Fig. 8a,b). Three very different scaling effects are observed in the configurations with a single perturbed parameter. For parameter 3 (*001*), the scaling is nonlinear: the USF increases between 10% and 20% CV but then decreases at 40% CV. The trend for parameter 2 (*010*) is a monotonic decrease in USF with increasing input uncertainty. Parameter 1 (*100*) actually attenuates uncertainty (negative USF) at the lower level of input CV but switches to uncertainty amplification at higher levels. The dominant trend of uncertainty scaling in those configurations with multiple perturbed parameters follows that observed for parameter 2 in isolation (*010*): decreasing USF with increasing input CV. Moreover, the pattern of USFs across model configurations is strikingly similar for both abundance and spatial autocorrelation. This similarity may be a product of the density-dependent controls; specifically, greater parameter variation leads to

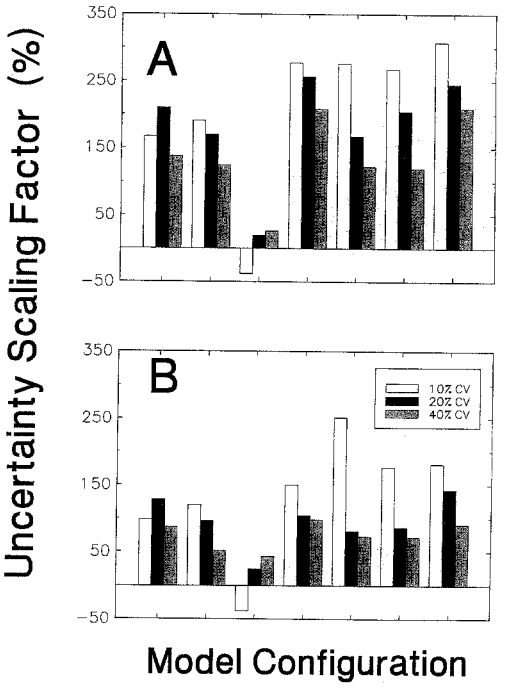

Fig. 8. Uncertainty scaling factors (USFs) for (a) abundance and (b) spatial autocorrelation.

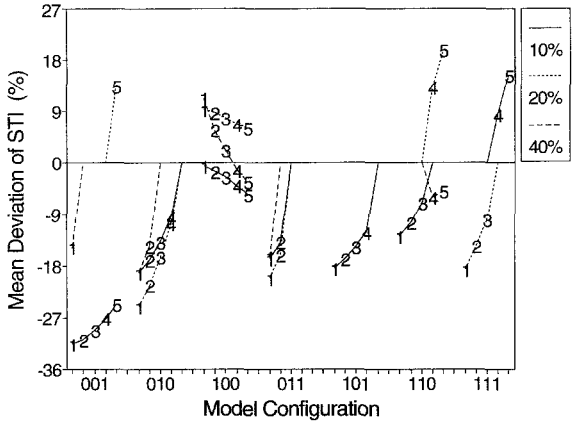

Fig. 9. Effect of parameter uncertainty on spatio-temporal autocorrelation as a function of lag distance. Numbers denote lag at which significant *STI* scores occur.

more "extreme" results that are effectively censored by the density-dependent functions.

3.5. Nonlinearity of spatio-temporal effects

To this point only nearest-neighbor spatial effects have been examined. What effects are discernible at spatial lags greater than one? As the most significant deviations have been observed in the spatio-temporal autocorrelation (Fig. 7), it is appropriate to examine higher-order lag patterns in *STI*. Fig. 9 displays results of the normalized mean *STI* scores observed at lags 1 to 5 along the 8 principal axes (queen's case) for each model configuration; deviations not significantly different from the reference are plotted as zero.

Three patterns are notable. First, the effects are highly nonlinear across lags and uncertainty levels. Note, for instance, the patterns of configuration *110*. At low uncertainty, significant negative deviations decrease in magnitude from lags 1 to 3 and are not significant for lags 4 and 5. In contrast, only lags 4 and 5 are significant at higher uncertainty levels; yet, at 20% CV the deviations are positive but they are negative at 40% CV. Second, only configuration *100* retains significant effects across lags and uncertainty levels. Here again, however, the nonlinearity is striking. At low uncertainty the magnitude of the deviation becomes more negative with lag distance. At 20% CV, the slope of the lag pattern is comparable but the deviation becomes less positive with lag. The slope of the lag pattern becomes substantially steeper at 40% CV with deviations moving from positive to negative as a function of lag. Third, the slopes of the lag patterns for the density-dependent parameters (*001*, *010*) are generally opposed to those for the explicitly spatial parameter (*100*), indicating that very different forms of spatio-temporal influence arise from these parameters. From an overall consideration of spatio-temporal effects, it could be concluded that while density dependent parameters are more sensitive in terms of magnitude of deviation, the spatial parameter exerts an effect that is small in absolute deviation but one that is pervasive and consistently significant.

4. Discussion and conclusion

How do the autocorrelation indices compare with other methods proposed for spatial simulation models? Turner et al. (1989) reviewed three groups of model performance indices that are well-suited for lattice (gridcell) data: (1) indices of spatial pattern, including fractal dimension, contagion, adjacency, and interface; (2) a spatial predictability index developed from Colwell (1974); and (3) a multiple resolution goodness of fit procedure described by Costanza (1989). This grouping reflects the lineage of the indices rather than their mechanism. A more appropriate functional grouping distinguishes between geometry-based measures (fractal dimension, interface) and probability-based measures, with the latter category separating frequency-based measures (adjacency, multiple resolution procedure) from information-theoretic measures (contagion, spatial predictability). The probability-based measures are directly affected by spatial autocorrelation: the spatial transition probabilities that underlie adjacency, contagion, and spatial predictability measures are, by definition, strongly correlated with spatial autocorrelation. The window-based frequency approach of the multiple resolution procedure is likewise sensitive to spatial autocor-

relation but does not quantify it. The geometry-based measures are also affected by spatial autocorrelation, albeit indirectly, e.g., strong negative autocorrelation can induce more edges, more patchiness.

Furthermore, each of the techniques in Turner et al. (1989) was demonstrated only using multinomial (categorical) data and, while they can be used with ordinal data, few can be readily adapted to interval-scaled data. The autocorrelation indices presented here, on the other hand, pertain to interval data and, with minor modifications, to ordinal data, and analogous indices exist for categorical data (Cliff and Ord, 1981a).

A more substantial limitation of the techniques in Turner et al. (1989) is a lack of mechanisms for testing statistical significance. At what point are two fractal dimensions considered significantly different? Is this breakpoint globally consistent or distinctive to each dataset? What are the moments of the sampling distribution of the multiple resolution procedure or contagion indices? While permutation/resampling methods can be employed (Costanza, 1989; Manly, 1989), they may yield computationally unwieldy results. The spatio-temporal error analysis described in this paper exercised a Cray Y-MP; if map-level permutations to assess spatial index significance were nested within the Monte Carlo simulations, the computational burden could easily grow by more than an order of magnitude. Autocorrelation indices have sampling distributions with well-defined, readily calculable moments as well as weighting matrices within which to embed testable hypotheses about spatial and spatio-temporal relatedness.

Finally, a problem shared by every technique mentioned here, including autocorrelation indices, is the problem of nonstationarity in spatial and spatio-temporal data. Stationarity and its absence, nonstationarity, describe the behavior of the probability distributions generated by random functions (or random fields) through space and/or time. The basic concept of stationarity is that of consistency: the probability distributions (and their moments) do not change with respect to the index set, where the index set denotes some collection of dimensional referents, e.g., continuous points in space, discrete time lags, spatio-temporal increments. Stationarity has many shades of definition and the reader is referred to the brief but helpful discourse in Cressie (1991). The existence of stationarity or rather the assumption of stationarity is critical for statistical inference simply because it is difficult to hit a shifting target. Unfortunately for estimation and prediction, the lack of stationarity is the norm in spatial data; indeed, as noted above, spatial nonstationarity has many guises, e.g. anisotropies, gradients, waves, patchiness, nested effects.

How does nonstationarity impact the indices proposed for spatial model error analysis? The probability-based measures of spatial pattern (contagion, adjacency, spatial predictability, multiple resolution procedure) make an implicit assumption of spatial stationarity when frequency data collected across the study region (e.g., image) is normalized by number of sample sites (e.g., pixels). The multiple resolution procedure may be more robust to nonstationarity because it sums local deviations from a reference across a variety of scales. However, because it is likely that serious deviations in model predictions will be manifest in spatio-temporal clusters rather than in a consistent bias or random noise, the multiple resolution procedure may too fall prey to the confounding effects of nonstationarity. The geometry-based measures (fractal dimension, interface) may be robust to nonstationarity but only because expectations about their sampling distributions are so ill-defined.

Autocorrelation indices are also susceptible to nonstationarity. Both Moran's I and Griffith's STI assess deviations from a global mean; the implicit assumption is that the mean represents the one probability distribution that pertains to any (space–time) location in the study region. This assumption is too strong for many situations but there are some ways to attempt to remove nonstationarity from the data. First, data which are filtered to remove trends often leave residuals that are stationary. Both parametric trend surface removal and non-parametric median polish procedures have proven successful in attenuating spatial nonstationarity (Cressie, 1991). Second, some spatial statistics assume intrinsic stationar-

ity, i.e., stationary distributions exist for increments of the index set, rather than a single global distribution. The success of geostatistics has been built upon this idea (Cressie, 1991), but the assumption of intrinsic stationarity does not eliminate the problem of nonstationarity. Third, the data may amenable to partitioning into quasi-stationary segments. This approach is commonly used to handle spatial anisotropies. This method was employed here successfully to avoid the model's initial transient (generations 1–4) in autocorrelation calculations. Such partitioning, however, requires some prior knowledge about how the data are structured. Indeed, many of the assumptions in statistical methods arise from a fundamental ignorance about the dynamical behavior of the system under consideration. The more we know about a system, the more precisely we can phrase our hypotheses. The challenge for spatial model error analysis remains the development of algorithms and measures that are at once sensitive to significant changes in spatio-temporal patterns and robust to assumptions about nonstationarity. The research presented here worked with a stochastic dynamic model unfolding on an isotropic gridscape. The next phase of research must probe the performance of autocorrelation indices in the more complicated and realistic context of anisotropic environments and in model fitting of actual spatial datasets.

Parameter uncertainty in a spatial simulation can induce a stunning range of complex spatio-temporal effects. The results presented here demonstrate both the need for tools to conduct error analysis in spatial simulation models and the ability of autocorrelation indices to address this need. Autocorrelation indices are not a panacea but a readily accessible beginning to the rather involved business of simulating ecological systems that exhibit complex dynamics in time and space.

Acknowledgements

I would like to thank A. Braga-Henebry, T.L. Benning, T.R. Seastedt for their advice, assistance, and encouragement during various phases of this research. The manuscript benefitted from readings by W.K. Dodds and C.L. Turner. Access to high performance computing platforms was provided under grants *wjo* and *ufb* by the National Center for Supercomputing Applications, University of Illinois at Urbana-Champaign. This research was funded under NSF grant BSR-9011662, Long Term Ecological Research at Konza Prairie.

Appendix 1

Equation for second moment of Griffith's *STI* under normality assumption.

$$E(STI^2) = \left[(T-1)^2(2n^2T^2A - 4nTB + 3C)\right] \times * \left[T^2(nT-1)(nT+1)C\right]^{-1}$$

where

$$A = \sum_{t=2}^{t=T}\sum_{i=1}^{i=n}\sum_{j=1}^{j=n} w_{ijt-1}^2$$

$$B = \sum_{i=1}^{i=n}\left(\sum_{t=2}^{t=T}\sum_{j=1}^{j=n} w_{ijt-1}\right)^2$$

$$C = \left(\sum_{t=2}^{t=T}\sum_{i=1}^{i=n}\sum_{j=1}^{j=n} w_{ijt-1}\right)^2$$

where n is the number of areal units, T is the number of temporal units, w_{ijt} is a spatio-temporal weighting. Note that the variance of *STI* under the normality assumption depends only upon the weighting scheme and the number of samples.

References

Anselin, L., 1988. Spatial Econometrics: Methods and Models. Kluwer, Dordrecht, 284 pp.

Arbia, G., 1989. Spatial Data Configuration in Statistical Analysis of Regional Economic and Related Problems. Kluwer, Boston, 256 pp.

Barbour, A.D. and Eagleson, G.K., 1986. Tests for space–time clustering. In: P. Tautu (Editor), Stochastic Spatial Processes, Lecture Notes in Mathematics, No. 1212. Springer-Verlag, New York, pp. 42–51.

Beck, M.B., 1987. Water quality modeling: a review of the analysis of uncertainty. Water Resour. Res., 23: 1393–1442.

Cale, W.G. and Odell, P.L., 1980. Behaviour of aggregate state variables in ecosystem models. Math. Biosci., 49: 121–137.

Cale, W.G., Henebry, G.M. and Yeakley, J.A., 1989. Inferring process from pattern in natural communities. BioScience, 39: 600–605.

Chadderton, R.A., Miller, A.C. and McDonnell, A.J., 1982. Uncertainty analysis of dissolved oxygen model. J. Environ. Eng. Div., 108: 1003–1013.

Chou, Y.-H., Minnich, R.A., Salazar, L., Power, J.D. and Dezzani, R.J., 1990. Spatial autocorrelation of wildfire distribution in the Idyllwild quadrangle, San Jacinto mountain, California. Photogram. Eng. Remote Sens., 56: 1507–1513.

Cliff, A.D. and Ord, J.K., 1981a. Spatial Processes: Models and Applications. Pion, London, 266 pp.

Cliff, A.D. and Ord, J.K., 1981b. Spatial and temporal analysis: autocorrelation in space and time. In: N. Wrigley and R.J. Bennett (Editors), Quantitative Geography: A British View. Routledge and Kegan Paul, London, pp. 104–110.

Colwell, R.K., 1974. Predictability, constancy, and contingency of periodic phenomena. Ecology, 55: 1148–1153.

Costanza, R., 1989. Model goodness of fit: a multiple resolution procedure. Ecol. Model., 47: 199–215.

Costanza, R. and Maxwell, T., 1991. Spatial ecosystem modelling using parallel processors. Ecol. Model., 58: 159–183.

Costanza, R., Sklar, F.H. and White, M.L., 1990. Modeling coastal landscape dynamics. BioScience, 40: 91–107.

Cressie, N.A.C., 1991. Statistics for Spatial Data. Wiley, New York, 900 pp.

Forman, R.T.T. and Godron, M., 1986. Landscape Ecology. Wiley, New York, 619 pp.

Gardner, R.H., Cale, W.G. and O'Neill, R.V., 1982. Robust analysis of aggregation error. Ecology, 63: 1771–1779.

Golub, G.H., 1993. Scientific Computing: An Introduction With Parallel Computing. Academic, Boston, 442 pp.

Griffith, D.W., 1981. Interdependence of space and time: numerical and interpretative considerations. In: D. Griffith and R. MacKinnon (Editors), Dynamic Spatial Models. Sijthoff and Noordhoff, Alphen a/d Rijn, pp. 258–287.

Henebry, G.M., 1989. Assessing model reliability under parameter uncertainty: applications to ecology and pharmacokinetics. Unpublished Ph.D. Dissertation, The University of Texas at Dallas, 376 pp.

Hillis, W.D., 1986. The Connection Machine. MIT Press, Cambridge, 190 pp.

Hillis, W.D. and Boghosian, B.M., 1993. Parallel scientific computation. Science, 261: 856–871.

Hornberger, G.M. and Spear, R.C., 1981. An approach to the preliminary analysis of environmental systems. J. Environ. Manage., 12: 7–18.

Huston, M., DeAngelis, D. and Post, W., 1988. New computer models unify ecological theory. BioScience, 38: 682–691.

Klauber, M.R., 1975. Space–time clustering analysis: a prospectus. In: D. Ludwig and K.L. Cooke (Editors), Epidemiology. Society for Industrial and Applied Mathematics, Philadelphia, pp. 75–89.

King, A.W., 1991. Translating models across scales in the landscape. In: M.G. Turner and R.H. Gardner (Editors), Quantitative Methods in Landscape Ecology. Springer-Verlag, New York, pp. 479–517.

King, A.W., Johnson, A.R. and O'Neill, R.V., 1991. Transmutation and functional representation of heterogeneous landscapes. Landsc. Ecol., 5: 239–253.

Knox, G., 1964. The detection of space–time interactions. Appl. Stat., 13: 25–29.

Manly, B.F.J., 1989. Randomization and Monte Carlo Methods in Biology. Chapman and Hall, London, 281 pp.

Mantel, N., 1967. The detection of disease clustering and a generalized regression approach. Cancer Res., 27: 209–220.

Moran, P.A.P., 1950. Notes on continuous stochastic phenomena. Biometrika, 37: 17–23.

Murray, J.D., 1990. Mathematical Biology. Springer-Verlag, New York, 767 pp.

O'Neill, R.V., 1979. Transmutations across hierarchical levels. In: G.S. Innis and R.V. O'Neill (Editors), Systems Analysis of Ecosystems. International Cooperative Publishing House, Fairland, MD, pp. 58–78.

O'Neill, R.V., DeAngelis, D.L., Waide, J.B. and Allen, T.F.H., 1986. A Hierarchical Concept of Ecosystems. Princeton University Press, Princeton, NJ, 254 pp.

Openshaw, S., 1977. A geographical solution to scale and aggregation problems in region-building, partitioning and spatial modelling. Trans. Inst. Br. Geogr. New Ser., 2: 459–475.

Openshaw, S. and Taylor, P.J., 1981. The modifiable unit area problem. In: N. Wrigley and R.J. Bennett (Editors), Quantitative Geography: a British view. Pion, London, pp. 127–144.

Rastetter, E.B., King, A.W., Cosby, B.J., Hornberger, G.M., O'Neill, R.V. and Hobbie, J.E., 1992. Aggregating fine-scale ecological knowledge to model coarser-scale attributes of ecosystems. Ecol. Appl., 2: 55–70.

Ripley, B.D., 1988. Statistical Inference for Spatial Processes. Cambridge University Press, New York, 148 pp.

Rosswall, T., Woodmansee, R.G. and Risser, P.G., 1988. Scales and Global Change, SCOPE 35. Wiley, New York, 355 pp.

Scavia, D., Powers, W.F., Canale, R.P. and Moody, J.L., 1981. Comparison of first-order error analysis with Monte Carlo simulation in time-dependent lake eutrophication models. Water Resour. Res., 17: 1051–1059.

Selvin, S., 1991. Statistical Analysis of Epidemiologic Data. Oxford University Press, New York, 375 pp.

Siemiatycki, J., 1978. Mantel's space–time clustering statistic: computing higher moments and a comparison of various data transforms. J. Stat. Comput. Simul., 7: 13–31.

Sklar, F.H. and Costanza, R., 1991. The development of dynamic spatial models for landscape ecology: a review and prognosis. In: M.G. Turner and R.H. Gardner (Editors), Quantitative Methods in Landscape Ecology. Springer-Verlag, New York, pp. 239–288.

Sokal, R.R. and Oden, N.L., 1978a. Spatial autocorrelation in biology 1. Methodology. Biol. J. Linnean Soc., 10: 199–228.

Sokal, R.R. and Oden, N.L., 1978b. Spatial autocorrelation in biology 2. Some biological implication and four applications of evolutionary and ecological interest. Biol. J. Linnean Soc., 10: 229–249.

Soulé, M.E., 1986. Conservation Biology: The Science of Scarcity and Diversity. Sinauer, Sunderland, MA, 584 pp.

Soulé, M.E., 1991. Conservation: tactics for a constant crisis. Science, 253: 744–750.

Turner, M.G., 1989. Landscape ecology: the effect of pattern on process. Annu. Rev. Ecol. Syst., 20: 171–197.

Turner, M.G., Constanza, R. and Sklar, F.H., 1989. Methods to evaluate the performance of spatial simulation models. Ecol. Model., 48: 1–18.

Upton, G.J.G. and Fingleton, B., 1985. Spatial Data Analysis by Example, Volume I: Point Pattern and Quantitative Data. John Wiley, New York, 410 pp.

Warwick, J.J. and Cale, W.G., 1986. Effects of parameter uncertainty in stream modeling. J. Environ. Eng., 112: 479–489.

Warwick, J.J. and Cale, W.G., 1988. Estimating model reliability using data with uncertainty. Ecol. Model., 41: 169–181.